Research Square

Preprints are preliminary reports that have not undergone peer review.
They should not be considered conclusive, used to inform clinical practice,
or referenced by the media as validated information.

# ECM1 is upregulated in chronic ocular Stevens–Johnson syndrome and promotes inflammatory, adhesive and angiogenic responses in vitro

**Kartik Goel**
Manipal Academy of Higher Education
**Monika Chouhan**
Dr. Shroff's Charity Eye Hospital
**Navjot Marwah**
Manipal Academy of Higher Education
**Aastha Garg**
Dr. Shroff's Charity Eye Hospital
**Abha Gour**
Dr. Shroff's Charity Eye Hospital
**Mehak Sapra**
vohramehak04@gmail.com

Dr. Shroff's Charity Eye Hospital
**Virender Singh Sangwan**
Dr. Shroff's Charity Eye Hospital
**Anil Tiwari**
Dr. Shroff's Charity Eye Hospital

**Article**

**Keywords:** Stevens–Johnson syndrome, ECM1, extracellular matrix remodeling, ocular surface, conjunctiva, inflammation

**Posted Date:** November 12th, 2026

**DOI:** https://doi.org/10.21203/rs.3.rs-11128676/v1

**License:** This work is licensed under a Creative Commons Attribution 4.0 International License.
Read Full License

**Additional Declarations:** No competing interests reported.

# ECM1 is upregulated in chronic ocular Stevens–Johnson syndrome and promotes inflammatory, adhesive and angiogenic responses in vitro

Kartik Goel[1,2], Monika Chouhan[3], Navjot Marwah[1,2], Virender Sangwan[1,4,5], Aastha Garg[4], Abha Gour[1,4,5], Anil Tiwari[1,4,5]*, Mehak Sapra[1,4,5]*

1. *Eicher-Shroff Centre for Stem Cell Research, Dr. Shroff's Charity Eye Hospital, 5027, Kedarnath Lane, Daryaganj, New Delhi 110002, India*
2. *Centre for Doctoral Studies, Manipal Academy for Higher Education, Manipal, Karnataka, India*
3. *Shroff – Pandorum Centre for Ocular Regeneration (SPCORE), Dr. Shroff's Charity Eye Hospital, 5027, Kedarnath Lane, Daryaganj, New Delhi 110002, India*
4. *Cornea Department, Dr Shroff's Charity Eye Hospital, 5027, Kedarnath Lane, Daryaganj, New Delhi 110002, India*
5. *Centre for unknown and rare disease (CURED), Dr Shroff's Charity Eye Hospital, 5027, Kedarnath Lane, Daryaganj, New Delhi 110002, India*

**Corresponding Author**:

**Dr Mehak Sapra, Eicher-Shroff Centre for Stem Cell Research, Dr. Shroff's Charity Eye Hospital, 5027, Kedarnath Lane, Daryaganj, New Delhi 110002, India* , vohramehak04@gmail.com

**Dr Anil Tiwari, Eicher-Shroff Centre for Stem Cell Research, Dr. Shroff's Charity Eye Hospital, 5027, Kedarnath Lane, Daryaganj, New Delhi 110002, India* , tiwaria1228@gmail.com

**Abstract**

Chronic ocular Stevens–Johnson syndrome (SJS) is characterized by persistent inflammation, conjunctival fibrosis, and progressive ocular surface dysfunction, but the molecular mechanisms underlying extracellular matrix (ECM) remodeling remain poorly understood. We characterized the conjunctival transcriptomic landscape of chronic ocular SJS and investigated the functional relevance of extracellular matrix protein 1 (ECM1). Bulk RNA sequencing was performed on conjunctival tissues from patients with chronic ocular SJS (n = 5) and healthy controls (n = 4), followed by differential expression and pathway enrichment analyses. ECM1 was further validated by quantitative real-time PCR, immunofluorescence, and ELISA, while gelatin zymography was used to assess matrix metalloproteinase activity. Transcriptomic profiling revealed marked dysregulation of inflammatory and ECM-associated pathways, with ECM1 among the prominently upregulated genes. Recombinant ECM1 treatment of human conjunctival epithelial cells increased expression of pro-inflammatory mediators, including IL1B, IL1A, IL6, and IL36G, together with ECM remodeling-associated genes. ECM1 exposure also enhanced cell adhesion and angiogenic responses in vitro. These findings identify ECM1 as a potential mediator linking inflammation, ECM remodeling, and angiogenic responses in chronic ocular SJS and support further investigation of ECM1-associated pathways as potential therapeutic targets.

Keyword: *Stevens–Johnson syndrome; ECM1; extracellular matrix remodeling; ocular surface; conjunctiva; inflammation*.

## 1. INTRODUCTION

Stevens–Johnson syndrome is a severe immune-mediated mucocutaneous disorder associated with substantial ocular morbidity and long-term vision-threatening complications[1] . Chronic ocular

sequelae affect a significant proportion of patients and include persistent inflammation, conjunctival cicatrization, dry eye disease, limbal stem cell deficiency, corneal neovascularization, keratinization, and progressive ocular surface failure[2,3]. Persistent immune dysregulation, aberrant epithelial differentiation, and chronic inflammatory signalling are increasingly recognized as key drivers of ongoing ocular surface damage long after resolution of the acute disease episode[4,5].

Traditionally, chronic ocular Stevens–Johnson syndrome (SJS) has been viewed largely as a residual cicatricial sequela of the acute disease phase[6–8]. However, growing evidence suggests that chronic ocular SJS represents an active and progressive inflammatory disorder characterized by persistent immune activation and ongoing tissue remodelling[7,9–13]. Histopathological studies have demonstrated chronic inflammatory infiltrates comprising T cells, macrophages, and Langerhans cells, along with basement membrane disruption and vasculitis alterations within the conjunctiva[6,12,14]. Long-term clinical follow-up studies further indicate that progressive conjunctival cicatrization, recurrent inflammatory episodes, and ocular surface failure may continue years after the initial acute insult, highlighting the dynamic and sustained nature of chronic ocular surface pathology in SJS[6,15].

Extracellular matrix (ECM) remodeling is central to tissue repair, fibrosis, angiogenesis, and epithelial homeostasis across ocular surface diseases[16,17]. Dysregulated ECM deposition and degradation can profoundly alter stromal architecture, inflammatory signaling, cell adhesion, and corneal transparency[10]. Multiple ocular transcriptomic and fibrosis studies have identified enrichment of ECM-associated pathways involving fibronectin (FN1), matrix metalloproteinases (MMPs), collagens, tenascin-C (TNC), integrins, and transforming growth factor-β (TGF-β)-associated signaling[10,18,19]. Myofibroblast differentiation and persistent stromal activation are

increasingly recognized as major contributors to chronic ocular fibrosis and pathological wound healing[10,18,20].

Recent advances in bulk and single-cell transcriptomics have provided important insights into ECM-associated molecular alterations across ocular diseases including keratoconus, corneal fibrosis, Fuchs endothelial corneal dystrophy, and ocular mucous membrane pemphigoid [10,19,21–23]. These studies consistently demonstrate dysregulation of pathways related to ECM organization, collagen biosynthesis, inflammatory signaling, angiogenesis, and stromal-epithelial communication. Notably, conjunctival transcriptomic profiling in ocular mucous membrane pemphigoid identified strong enrichment of profibrotic ECM remodeling pathways, highlighting the importance of ECM-associated molecular networks in chronic ocular surface scarring disorders[19].

Extracellular matrix protein 1 (ECM1) is a secreted glycoprotein involved in ECM organization, inflammatory regulation, angiogenesis, epithelial differentiation, and cell adhesion[24]. ECM1 interacts with multiple ECM-associated molecules including fibronectin, laminins, and matrix metalloproteinases, and has been implicated in fibrosis, chronic inflammation, and tissue remodeling across systemic diseases[25–30]. Recent studies have demonstrated that ECM1 promotes inflammatory and fibrotic responses through modulation of macrophage polarization, TGF-β activation, fibroblast activation, and extracellular matrix-associated signaling pathways[26,27,30]. Despite its emerging importance in fibrosis biology, the role of ECM1 in ocular surface disease and chronic ocular SJS remains poorly understood.

In the present study, we performed bulk RNA sequencing of conjunctival tissues from patients with chronic ocular SJS and healthy controls to characterize the transcriptomic landscape associated with chronic disease. Through differential expression and pathway enrichment analyses,

ECM1 emerged as a significantly dysregulated ECM-associated molecule. We further investigated the functional role of ECM1 using patient tissue validation and in vitro assays to evaluate its contribution to inflammatory, angiogenic, adhesive, and extracellular matrix-associated responses in chronic ocular SJS.

## 2. Results

### 2.1 Transcriptomic profiling reveals ECM Remodeling dysregulation in chronic ocular Stevens–Johnson syndrome

The RNA-sequencing cohort comprised five chronic ocular SJS samples and four healthy controls. Detailed demographic and clinical characteristics are provided in (Supplementary Table 1). Bulk RNA sequencing of conjunctival tissues from chronic ocular Stevens–Johnson syndrome (SJS) patients and healthy controls revealed extensive transcriptomic alterations associated with chronic ocular surface disease (Fig. 1A). Differential gene expression analysis identified 2978 significantly dysregulated genes (adjusted p-value $< 0.05$) between diseased and healthy conjunctival tissues, with clear segregation observed between the two groups (Fig. 1B–C). Several ECM-associated and inflammatory genes, including ECM1, TNC, GJB2, SLC24A3, and AKR1B10, were significantly upregulated in chronic ocular SJS conjunctiva, while multiple epithelial and homeostatic genes were comparatively downregulated (Fig. 1B). Among the most highly upregulated ECM-associated genes, ECM1 emerged as a particularly compelling candidate due to its marked upregulation, association with ECM organization pathways, and previously reported roles in inflammation, fibrosis, angiogenesis, and tissue remodeling. Given that the contribution of ECM1 to chronic ocular surface disease remains poorly understood, it was selected for downstream validation and functional characterization. Transcriptomic visualization and

downstream analyses were performed using the top 500 significantly dysregulated genes. Hierarchical clustering and heatmap analysis demonstrated distinct transcriptomic signatures between healthy and diseased conjunctival tissues, highlighting widespread molecular remodelling in chronic ocular SJS (Fig. 1C).

Gene Set Enrichment Analysis (GSEA) demonstrated significant enrichment of pathways associated with ECM organization, collagen-containing ECM, ECM structural constituents, integrin binding, cytokine activity, cytokine receptor binding, receptor-ligand signalling, cell-cell adhesion, gap junction activity, protease binding, and growth factor activity in diseased conjunctival tissues (Fig. 1D). Additional enrichment of pathways related to ECM-receptor interaction, collagen biosynthesis and degradation, ECM proteoglycans, complement and coagulation cascades, keratinization, cornified envelope formation, neutrophil degranulation, epithelial differentiation, and cytoskeletal remodelling further supported the presence of extensive inflammatory and epithelial remodeling in chronic ocular SJS. GO cellular component analysis demonstrated enrichment of ECM, basement membrane, collagen-containing ECM, keratin filament, desmosome, and cell-cell junction-associated pathways, while GO molecular function analysis identified significant enrichment of cytokine activity, receptor regulator activity, collagen binding, glycosaminoglycan binding, integrin binding, and ECM structural constituent pathways. Reactome pathway analysis further demonstrated enrichment of ECM organization, integrin cell surface interactions, collagen assembly pathways, keratinization, neutrophil degranulation, and gap junction trafficking pathways. In contrast, downregulated pathways were predominantly associated with transmembrane transporter activity and ion transport-related functions (Supplementary Figure 1–5). Collectively, these findings indicate that chronic ocular SJS is

characterized by extensive inflammatory transcriptomic remodeling involving persistent ECM dysregulation, inflammatory activation, epithelial stress responses, and altered tissue homeostasis.

**2.2 Validation of ECM remodeling and inflammatory dysregulation in chronic ocular Stevens–Johnson syndrome tissues**

Given the strong enrichment of extracellular matrix-associated pathways identified through transcriptomic analysis, further validation of ECM remodeling-associated genes was performed in chronic ocular SJS conjunctival tissues (Fig. 2A). Heatmap analysis demonstrated increased expression of multiple ECM remodeling-associated genes in diseased conjunctiva compared to healthy controls. qRT-PCR validation confirmed significant upregulation of extracellular matrix-associated genes including ECM1, TNC, FN1, αSMA, MMP3, MMP9, PAI1, and TGFβ1 in chronic ocular SJS conjunctival tissues (Fig. 2B). These findings support activation ECM remodeling, fibrosis-associated signaling, and tissue remodeling pathways within the chronic ocular SJS microenvironment.

Protein-level validation further demonstrated increased ECM1, FN1, and TNC expression in diseased conjunctival tissues by immunofluorescence staining compared to healthy controls (Fig. 2C). Increased staining intensity was observed within both epithelial and stromal compartments, suggesting widespread ECM remodeling across the conjunctival tissue architecture. Quantification of mean fluorescence intensity further confirmed significantly elevated protein expression in chronic ocular SJS tissues. ELISA-based analysis demonstrated significantly increased tear levels of inflammatory and extracellular matrix-associated proteins including TNFα, IL1β, ECM1, and TNC in chronic ocular SJS samples compared to controls (Fig. 2D). Gelatin zymography additionally demonstrated increased secretory matrix metalloproteinase activity in diseased tear samples, consistent with active ECM turnover and proteolytic remodeling within the ocular surface

160 microenvironment (Fig. 2E) (Supplementary Figure 6). Together, these findings validate the
161 transcriptomic evidence of persistent ECM remodeling and inflammatory dysregulation in chronic
162 ocular SJS.
163
164 **2.3 ECM1 promotes inflammatory responses in conjunctival epithelial cells**
165 To investigate the functional role of ECM1 in ocular surface inflammation, recombinant ECM1
166 protein treatment was performed in human conjunctival epithelial cells (HCjE) followed by
167 downstream molecular analyses (Fig. 3A) (Supplementary Figure 7). ECM1 treatment resulted in
168 significant upregulation of multiple inflammatory mediators including TNFα, IL6, IL8, IL1A,
169 IL1β, and IL36γ compared to untreated controls (Fig. 3B). In addition, epithelial stress-associated
170 inflammatory mediators including S100A7, S100A8, and S100A9 were significantly increased
171 following ECM1 exposure, suggesting activation of epithelial inflammatory and stress-response
172 pathways. Protein-level validation further demonstrated increased secretion of IL1β and TNFα
173 following ECM1 treatment in HCjE cells (Fig. 3C). Collectively, these findings indicate that
174 ECM1 actively promotes inflammatory signaling within conjunctival epithelial cells and may
175 contribute to persistent ocular surface inflammation in chronic ocular Stevens–Johnson syndrome.
176 **2.4 ECM1 promotes adhesive and angiogenic responses**
177 To further evaluate ECM1-associated remodeling responses, functional adhesion and angiogenesis
178 assays were performed following ECM1 treatment (Fig. 4A). Cell adhesion assays demonstrated
179 significantly enhanced adhesive responses following ECM1 coated wells compared to negative
180 controls, with increased cellular attachment and spreading observed in ECM1-coated conditions
181 (Fig. 4B). These findings suggest that ECM1 may contribute to altered epithelial–matrix
182 interactions associated with chronic conjunctival remodelling and fibrosis. HUVEC tube

formation assays further demonstrated enhanced angiogenic responses following ECM1 treatment, characterized by increased capillary-like network formation and greater junction organization compared to untreated controls (Fig. 4C). Quantitative analysis demonstrated increased junction number and altered segment organization in ECM1-treated groups, supporting a potential role for ECM1 enhanced angiogenic activity in vitro. Collectively, these findings indicate that ECM1 functions beyond a transcriptomic marker and may actively contribute to ECM remodeling, adhesive responses, and angiogenic signaling in chronic ocular Stevens–Johnson syndrome.

## 3. Discussion

This study demonstrates that chronic ocular Stevens–Johnson syndrome is characterized by extensive fibrotic and inflammatory transcriptomic remodeling, involving ECM dysregulation, inflammatory signaling, and epithelial stress-associated pathways. Among the significantly altered genes, ECM1 emerged as a prominently upregulated extracellular matrix-associated mediator and was consistently validated at both transcript and protein levels in diseased conjunctival tissues. ECM1 was prioritized for further investigation because it was consistently associated with ECM remodeling signatures and represented a relatively unexplored mediator of ocular surface pathology. Importantly, Functional analyses demonstrated that recombinant ECM1 exposure altered inflammatory cytokine expression and cellular responses related to adhesion and angiogenesis in vitro, suggesting potential functional effects of ECM1 within the ocular surface microenvironment in chronic ocular SJS.

The strong enrichment of ECM organization, collagen-associated pathways, integrin interactions, and ECM structural constituent pathways highlights the central role of tissue remodeling in chronic ocular SJS pathology. In addition to classical inflammatory signaling, our findings suggest that

chronic ocular SJS involves persistent activation of inflammatory and epithelial remodeling programs that may contribute to progressive conjunctival cicatrization and ocular surface dysfunction.

Previously chronic ocular SJS has often been viewed as a static consequence of acute epithelial injury[31]. However, increasing evidence suggests that the chronic phase represents an active and progressive pathological process involving sustained immune dysregulation, abnormal epithelial repair, stromal remodeling, and persistent inflammatory activation[32]. Previous histopathological studies have demonstrated chronic inflammatory infiltrates, basement membrane disruption, vasculitis changes, and ongoing conjunctival immune activation even years following the acute episode[12]. Consistent with these observations, our transcriptomic analysis demonstrated robust enrichment of pathways associated with cytokine signaling, ECM organization, cell adhesion, receptor-ligand interactions, and protease activity, supporting the concept that chronic ocular SJS represents a continuously active inflammatory disease state rather than a residual scar phenotype alone.

A major finding of the present study was the strong enrichment of extracellular matrix-associated pathways and remodeling signatures within diseased conjunctival tissues.

Fibronectin and tenascin-C are particularly relevant in the context of chronic ocular surface remodeling. Fibronectin functions as a critical scaffold protein involved in cell adhesion, migration, and matrix assembly, while tenascin-C is associated with inflammatory tissue remodeling and stromal activation during chronic wound healing[17,18]. Similarly, elevated αSMA expression suggests myofibroblast activation and ongoing fibrotic transformation within diseased conjunctival tissues. Increased matrix metalloproteinase activity observed through zymography further supports active ECM turnover and tissue remodeling. Together, these findings

indicate that chronic ocular SJS conjunctiva exists in a persistently activated remodeling state characterized by simultaneous inflammatory signaling, matrix deposition, and matrix degradation. ECM1 emerged as a particularly compelling candidate due to its established roles in ECM organization, inflammation, angiogenesis, and tissue remodeling. Although ECM1 has been implicated in fibrosis and inflammatory regulation in several systemic diseases, its role in ocular surface disease remains largely unexplored.

In the present study, ECM1 demonstrated significant upregulation at both transcript and protein levels within chronic ocular SJS tissues. Immunofluorescence staining revealed enhanced ECM1 localization within epithelial compartment of diseased conjunctiva, suggesting broad involvement within the pathological ocular surface microenvironment. Importantly, transcriptomic enrichment analyses demonstrated strong association of ECM1 with ECM structural organization, cell adhesion, cytokine activity, and receptor-ligand signaling pathways, supporting its integration within broader fibro-inflammatory remodeling networks.

To further investigate the biological significance of ECM1, functional assays were performed using human conjunctival epithelial cells. Recombinant ECM1 treatment induced robust upregulation of multiple inflammatory mediators including IL1A, IL1β, IL6, IL8, TNFα, and IL36γ. These cytokines are known contributors to chronic ocular surface inflammation and epithelial stress responses and have previously been implicated in inflammatory amplification and tissue damage across ocular surface diseases. The observed induction of S100A7, S100A8, and S100A9 further suggests activation of epithelial stress-associated inflammatory pathways following ECM1 exposure. Collectively, these findings indicate that ECM1 may actively amplify inflammatory signaling within conjunctival epithelial cells and contribute to persistent ocular surface immune activation.

Interestingly, classical inflammatory cytokines were not among the most prominently validated transcriptomic alterations within conjunctival tissues themselves, despite increased inflammatory mediator expression observed following recombinant ECM1 treatment in conjunctival epithelial cells. This observation suggests that ECM1 may function as an upstream modulator capable of inducing secondary inflammatory responses within ocular surface epithelial cells rather than representing a purely inflammation-associated conjunctival transcriptomic marker. Furthermore, increased inflammatory protein levels identified in tear samples indicate that ECM1-associated inflammatory activity may involve broader ocular surface compartments beyond the conjunctiva alone. Beyond inflammation, ECM1 enhanced cellular adhesion and angiogenic responses, indicating potential roles in epithelial–matrix interactions, pathological wound healing, and ocular surface neovascularization. These findings suggest that ECM1 contributes to multiple aspects of chronic ocular surface remodeling in SJS.

The interplay between inflammation, ECM remodeling, and angiogenesis represents a central feature of chronic wound healing and fibrosis. Our findings position ECM1 at this critical intersection, where it may function as a molecular mediator linking epithelial inflammatory activation with stromal remodeling and vascular responses. Given previous evidence implicating ECM1 in TGF-β-associated fibrosis pathways, macrophage polarization, and matrix metalloproteinase regulation in systemic diseases, it is plausible that ECM1 contributes to maintenance of a chronic pathological remodeling niche in ocular SJS.

Our findings also align with emerging ocular transcriptomic studies demonstrating enrichment of extracellular matrix-associated molecular signatures across fibrotic and inflammatory ocular diseases. Similar dysregulation of FN1, collagens, MMPs, TNC, and ECM-associated pathways has been described in keratoconus, ocular mucous membrane pemphigoid, and corneal fibrosis

models. However, to our knowledge, the present study represents one of the first investigations specifically identifying and functionally characterizing ECM1 in chronic ocular surface disease associated with SJS.

The present study has several limitations. First, the transcriptomic analysis was performed in a relatively small cohort of conjunctival tissues, reflecting the rarity of chronic ocular Stevens–Johnson syndrome and the limited availability of surgical specimens. Although ECM1-associated transcriptional alterations were validated across independent patient cohorts using qRT-PCR, immunofluorescence, ELISA, and zymography, larger multi-center studies will be required to further confirm these findings. Second, while recombinant ECM1 induced inflammatory, adhesive, and angiogenic responses in vitro, mechanistic inhibition or loss-of-function studies were not performed and therefore the precise signaling pathways mediating ECM1-associated effects remain to be established. In addition, the present study did not include a chronic ocular SJS subgroup without conjunctival fibrosis, limiting our ability to determine whether ECM1 dysregulation is specifically associated with fibrotic remodeling rather than chronic ocular SJS more broadly. Third, the bulk RNA-sequencing approach lacks cell-type-specific resolution, and future studies employing single-cell or spatial transcriptomic technologies may provide deeper insight into the cellular sources and downstream targets of ECM1 within the ocular surface microenvironment. Additionally, while our findings suggest a pathogenic role for ECM1 in chronic ocular remodeling, the precise upstream regulators and downstream signaling pathways associated with ECM1-mediated responses remain to be elucidated. Future studies involving single-cell transcriptomics, spatial transcriptomics, and in vivo functional models may further clarify the cellular sources and mechanistic pathways associated with ECM1 in ocular surface disease. In particular, investigating the effects of ECM1 across different ocular surface cell populations,

including conjunctival epithelial cells, lacrimal and accessory gland-associated cells, stromal fibroblasts, and lymphoid or immune-associated tissues, may provide important insight into ECM1-mediated inflammatory regulation within chronic ocular SJS. Although immunofluorescence analysis in the present study demonstrated strong ECM1 localization within conjunctival epithelial compartments, the precise source of downstream inflammatory mediator release within the ocular surface microenvironment remains unclear and warrants further investigation.

Overall, the present study demonstrates that chronic ocular SJS is characterized by transcriptomic remodeling involving inflammation and extracellular matrix-associated pathways. ECM1 emerged as a significantly dysregulated mediator capable of promoting inflammatory, adhesive, and angiogenic responses, suggesting that ECM1 may actively contribute to persistent ocular surface remodeling and disease progression. These findings provide new insight into the molecular mechanisms underlying chronic ocular SJS and identify ECM1-associated pathways as potential therapeutic targets for future ocular surface interventions.

## 4. Methods

### 4.1 Study subjects and conjunctival tissue collection

Patients with chronic ocular Stevens–Johnson syndrome (SJS) attending the ophthalmology services at Dr. Shroff's Charity Eye Hospital, New Delhi, were recruited following written informed consent. Diagnosis was established based on documented clinical history and characteristic chronic ocular manifestations, including conjunctival cicatrization, keratinization, ocular surface inflammation, and corneal involvement. Disease severity was graded according to the Sotozono grading system. The original acute mucocutaneous diagnosis was recorded as SJS or toxic epidermal necrolysis (TEN); however, patients presenting with chronic ocular sequelae were

collectively classified as chronic ocular SJS for the purposes of the present study. Healthy conjunctival tissues obtained from individuals without ocular surface disease undergoing routine cataract surgery served as controls. Individuals with concurrent ocular infections or autoimmune ocular surface disorders were excluded.

The RNA-sequencing discovery cohort comprised conjunctival tissues from five patients with chronic ocular SJS and four healthy controls. An independent validation cohort comprising 20 patients with chronic ocular SJS and 10 healthy controls was used for downstream molecular validation. Clinical and demographic characteristics are provided in Supplementary Table 1.

Conjunctival tissues intended for RNA-based analyses were immediately preserved in RNAlater following collection. Tissue samples intended for histological analyses were fixed in formalin, while samples used for immunofluorescence were processed as fresh-frozen tissue blocks. The study was approved by the Institutional Ethics Committee of Dr. Shroff's Charity Eye Hospital (IRB/2025/MAR/09) and was conducted in accordance with the Declaration of Helsinki and all relevant institutional guidelines and regulations. Written informed consent was obtained from all participants before sample collection.

**4.2 Bulk RNA sequencing and transcriptomic analysis**

Bulk RNA sequencing was performed on conjunctival tissue samples from patients with chronic ocular SJS (n = 5) and healthy controls (n = 4). Total RNA was isolated from RNA (Invitrogen™ RNA*later*™ Stabilization Solution, Cat. No: AM7020) later-preserved conjunctival tissues using RNeasy Mini Kit (Qiagen, Cat no. / ID. 74104) and assessed for quantity and quality using 4200 TapeStation System (Agilient technologies ). Illumina Stranded Total RNA Prep, Ligation with Ribo-Zero Plus kit (Illumina, USA), incorporating ribosomal RNA depletion, according to the manufacturer's instructions. Libraries were subsequently sequenced on an Illumina NovaSeq 6000

platform using paired-end sequencing. Raw sequencing reads were assessed using FastQC and processed using Cutadapt and Trimmomatic to remove adapter sequences and low-quality reads. High-quality reads were aligned to the human reference genome GRCh38 using STAR, followed by gene-level quantification using feature Counts from the Subread package (GEO Acession no. **GSE350623**. **Direct link:** https://www.ncbi.nlm.nih.gov/geo/query/acc.cgi?acc=GSE350623; **Reviewer access token:** utknimakrxgpfuz). Differential gene expression analysis was performed using DESeq2 in R. Genes with an adjusted $P$ value < 0.05 were considered significantly differentially expressed. Multiple-testing correction was performed using the Benjamini–Hochberg method. Principal component analysis, hierarchical clustering, heatmaps and volcano plots were used to visualize transcriptomic differences between groups.

Functional enrichment analyses were performed using Gene Ontology, KEGG[33] and Reactome[34] databases to identify pathways associated with inflammation, extracellular matrix remodelling, fibrosis, angiogenesis and epithelial dysfunction. Protein–protein interaction networks were generated using the STRING database[35] .

**4.3 Quantitative real-time PCR**

Total RNA was isolated from conjunctival tissues from healthy controls (n = 10) and patients with chronic ocular SJS (n = 20), as well as from cultured cells used in functional experiments, using the RNeasy Mini Kit (Qiagen, Cat. No. 74104). Complementary DNA was synthesized using the RevertAid Reverse Transcription Kit (Thermo Scientific, Cat. No. K1691) according to the manufacturer's protocol. Conventional amplification steps associated with cDNA preparation were performed using a Bio-Rad T100 Thermal Cycler.

Quantitative real-time PCR was performed using PowerUp SYBR Green Master Mix (Applied Biosystems, Cat. No. A25742) on a Bio-Rad CFX Opus 96 Real-Time PCR System. The

amplification protocol consisted of an initial denaturation step at 90 °C for 3 min, followed by 40 cycles of denaturation at 90 °C for 10 s and annealing/extension at 60 °C for 20 s, followed by melt-curve analysis.

Expression of the ECM-associated and inflammatory genes *ECM1, FN1, TNC, ACTA2, MMP3, MMP9, SERPINE1, TGFB1, IL1A, IL1B, IL6, IL36G, TNF, S100A7, S100A8,* and *S100A9* was evaluated. Relative gene expression was calculated using the comparative Ct (2^−ΔΔCt) method following normalization to *GAPDH*. Primer sequences are provided in Supplementary Table 2.

**4.4 Tear protein extraction and ELISA**

Tear samples were collected using Schirmer strips from patients with chronic ocular SJS (n = 15) and healthy controls (n = 10). Following collection, tear proteins were extracted from each Schirmer strip using 60 µL phosphate-buffered saline supplemented with cOmplete Protease Inhibitor Cocktail (Roche, Cat. No. 11697498001). Samples were subsequently centrifuged to recover the extracted tear proteins. Total protein concentration in each tear extract was determined using the Pierce BCA Protein Assay according to the manufacturer's instructions. Equal amounts of total tear protein were used for subsequent ELISA measurements to minimize variability associated with differences in tear protein yield. Concentrations of ECM1 (BT-lab- Cat. No. E5270Hu), TNC (BT Lab, Cat. No. E1414Hu), IL-1β (BT Lab, Cat. No. E0143Hu) and TNF-α (BT Lab, Cat. No. E0082Hu) were quantified using commercially available ELISA kits according to the respective manufacturers' protocols. Cell-culture supernatants collected following ECM1 treatment were similarly analysed for IL-1β and TNF-α. Absorbance was measured at 450 nm using a BioTek Synergy H1 microplate reader (Agilent Technologies), and protein concentrations were calculated from the corresponding standard curves.

**4.5 Immunofluorescence staining and image analysis**

Fresh-frozen conjunctival tissue sections (5 μm) were mounted on positively charged glass slides and fixed with 4% paraformaldehyde. Sections were permeabilized using Triton X-100 and blocked with 5% bovine serum albumin to minimize non-specific binding.

Sections were incubated overnight at 4 °C with primary antibodies against ECM1 (Abclonal, Cat. No. A16368), FN1 (Millipore, Cat. No. AB2033) and TNC (Abclonal, Cat. No. A18156). Following primary antibody incubation, sections were washed with PBS containing 0.5% Tween-20 and incubated with Alexa Fluor 488-conjugated secondary antibody (Invitrogen, Catalog No A-11008) diluted 1:500 in 3% BSA for 1 h at room temperature in the dark. Nuclei were counterstained with DAPI (Sigma, Cat. No. D9542), and sections were mounted using antifade mounting medium (Cat. No. F4680).

Fluorescence images were acquired using a Carl Zeiss fluorescence microscope under identical acquisition and exposure settings for healthy and SJS samples. Mean fluorescence intensity was quantified using ImageJ following background subtraction and analysis of predefined regions of interest. For histopathological evaluation, formalin-fixed conjunctival tissues were routinely processed, paraffin-embedded, sectioned, and stained with hematoxylin and eosin. Sections were examined by light microscopy for epithelial morphology, inflammatory cell infiltration, and stromal tissue organization.

**4.6 Gelatin zymography**

Gelatin zymography was performed to assess matrix metalloproteinase activity in tear samples. Equal amounts of total tear protein, determined by Thermo Scientific™ Pierce™ BCA Protein Assay (Cat. No. 23225), were separated under non-reducing conditions on 10% polyacrylamide gels containing gelatin. Following electrophoresis, gels were incubated in renaturation buffer and

subsequently transferred to activation buffer to allow enzymatic degradation of the gelatin substrate. Following incubation, gels were stained and destained until areas of gelatinolytic activity became visible as clear bands against the stained background. Band intensities were quantified using ImageJ and expressed as relative densitometric units normalized to healthy controls.

### 4.7 Human conjunctival epithelial cell culture and ECM1 treatment

Immortalized human conjunctival epithelial cells (HCjE), kindly provided by Koji Kitazawa and colleagues and previously characterized[36] , were cultured according to the previously described protocol [36,37] . Cells were maintained in DMEM/F12 supplemented with B-27 Supplement (Gibco, Cat. No. 17504044), recombinant human FGF-7/KGF, Y-27632 dihydrochloride and antibiotics at 37 °C in a humidified atmosphere containing 5% $CO_2$. For functional experiments, HCjE cells were treated with recombinant human ECM1 protein (Cusabio, Cat. No. CSB-EP007383HU1) at 200 ng/mL for 24 h. Untreated cells served as controls. Following incubation, cells were harvested for qRT-PCR analysis and conditioned culture supernatants were collected for ELISA.

### 4.8 Cell adhesion assay

To evaluate HCjE adhesion to ECM1, 96-well culture plates were coated overnight at 4 °C with 100 µL recombinant human ECM1 at a concentration of 1 µg/mL. Collagen (Gibco™ Collagen I, rat tail, Cat. no. A1048301) coated wells served as positive controls, while 1ug/mL BSA-coated wells served as negative controls. Following coating, wells were blocked with 0.1% BSA before cell seeding. HCjE cells were seeded onto the coated surfaces and incubated for 4 h under standard culture conditions. Non-adherent cells were removed by washing with PBS. Adherent cells were

subsequently fixed and stained with crystal violet, and cell adhesion was quantified by measuring absorbance at 590 nm using a BioTek Synergy H1 microplate reader.

### 4.9 Endothelial tube formation assay

HiFi™ Human Umbilical Vein Endothelial Cells (HUVEC) (Cat. No. CL002) were used to assess the angiogenic response to ECM1. HUVECs were seeded onto Corning® Matrigel® Growth Factor Reduced (GFR) Basement Membrane Matrix (Cat. No. CLS354230) coated culture plates and treated with recombinant human ECM1 at 200 ng/mL and 400 ng/mL. Untreated cells served as controls. Following incubation, capillary-like network formation was visualized using phase-contrast microscopy. Images were analysed using ImageJ, and angiogenic parameters including junction number and segment length were quantified.

### 4.10 Statistical analysis

Statistical analyses were performed using GraphPad Prism and R statistical software. Data from experimental assays are presented as mean ± standard error of the mean (SEM). Non-parametric statistical tests were used for group comparisons. Comparisons involving two independent groups were performed using the Mann–Whitney U test. For transcriptomic analyses, $P$ values were adjusted for multiple testing using the Benjamini–Hochberg procedure, and adjusted $P$ values $< 0.05$ were considered statistically significant. All other statistical tests were two-sided, with $P < 0.05$ considered statistically significant.

## 5. Acknowledgements

The authors thank the clinical and research staff of Dr. Shroff's Charity Eye Hospital and the Eicher–Shroff Centre for Stem Cell Research for their assistance with patient recruitment,

sample collection, and technical support. The human conjunctival epithelial cell line used in this study was a kind gift from Prof. Shigeru Kinoshita. The authors also thank Koji Kitazawa, MD, PhD, Department of Ophthalmology, Kyoto Prefectural University of Medicine, Kyoto, Japan, for facilitating the provision of the cell line.

6. **Funding**: This work was supported by funding from Velux Stiftung (Project No. 1973), the DBT Ramalingaswami Fellowship, and the SHARE INDIA Pvt. Ltd. CSR Fund. Additional institutional support was provided by Dr. Shroff's Charity Eye Hospital and the Eicher Shroff Centre for Stem Cell Research.

7. **Commercial Relationships Disclosure**: K. Goel, None; M. Chouhan, None; N. Marwah, None; V. Sangwan, None; A. Garg, None; A. Gour, None; A. Tiwari, None; M. Sapra, None.

8. **Data Availability:** The RNA-sequencing datasets generated and analyzed during the current study have been deposited in the National Center for Biotechnology Information (NCBI) Gene Expression Omnibus (GEO) repository under accession number **GSE350623**. **Direct link:** https://www.ncbi.nlm.nih.gov/geo/query/acc.cgi?acc=GSE350623; **Reviewer access token:** utknimakrxgpfuz . Additional data supporting the findings of this study are available from the corresponding author upon reasonable request.

9.

10. **Author Contribution:** K.G. contributed to study design, experimental work, data acquisition, data analysis, interpretation of results, figure preparation, and manuscript drafting. M.C. and N.M. contributed to experimental work, sample processing, and data acquisition. V.S., A.Ga., and A.Go. contributed to clinical evaluation, patient recruitment, sample collection, and clinical interpretation of the findings. A.T. and M.S. conceived and supervised the study,

contributed to study design, data interpretation, and critical revision of the manuscript. All authors reviewed and approved the final manuscript.

## 11. References


1. Justice, J., Mukherjee, E., Martin-Pozo, M. & Phillips, E. Updates in the pathogenesis of SJS/TEN. *Allergol. Int.* **74**, 361 (2025).
2. Abrol, A., Gulanikar, A., Thakre, S. & Patel, A. Study of Ocular Manifestations of Stevens-Johnson Syndrome/Toxic Epidermal Necrolysis. *Indian Dermatol. Online J.* **11**, 570 (2020).
3. Stevens-Johnson Syndrome - EyeWiki. https://eyewiki.org/Stevens-Johnson_Syndrome.
4. Saeed, H. N. & Chodosh, J. Immunologic Mediators in Stevens-Johnson Syndrome and Toxic Epidermal Necrolysis. *Semin. Ophthalmol.* **31**, 85–90 (2016).
5. Abe, R. Immunological response in Stevens-Johnson syndrome and toxic epidermal necrolysis. *Journal of Dermatology* **42**, 42–48 (2015).
6. Basu, S. *et al.* Chronic Ocular Sequelae of Stevens-Johnson Syndrome in Children: Long-term Impact of Appropriate Therapy on Natural History of Disease. *Am. J. Ophthalmol.* **189**, 17–28 (2018).
7. Akgun, Z., Can, G. D. & Selver, O. B. Ocular involvement in Stevens–Johnson syndrome and toxic epidermal necrolysis: A review of current management and changing trends. *Indian J. Ophthalmol.* **73**, 1711–1722 (2025).
8. Gurumurthy, S., Iyer, G., Srinivasan, B., Agarwal, S. & Angayarkanni, N. Ocular surface cytokine profile in chronic Stevens-Johnson syndrome and its response to mucous membrane grafting for lid margin keratinisation. *British Journal of Ophthalmology* **102**, 169–176 (2018).
9. Hassanpour, K., Asadigandomani, H., Soltani Shahgoli, S., Amoozadehsamakoosh, A. & Soleimani, M. Ocular Complications in stevens-Johnson Syndrome and Toxic Epidermal Necrolysis: A Comprehensive Review. *Semin. Ophthalmol.* **41**, 356–370 (2026).
10. Kumar, R., Sinha, N. R., Jeffrey, M. T., Hofmann, A. C. & Mohan, R. R. Single-Cell Transcriptomics Shows Cellular Heterogeneity, Intercellular Communication, and Extracellular Matrix Remodeling in Corneal Fibrosis In Vivo. *Invest. Ophthalmol. Vis. Sci.* **66**, 48–48 (2025).
11. Ueta, M. *et al.* Severe ocular complications of SJS/TEN and associations among pre-onset, acute, and chronic factors: a report from the international ophthalmology collaborative group. *Front. Med. (Lausanne).* **10**, 1189140 (2023).
12. Liu, Y. *et al.* Ocular surface involvement and histopathologic changes in the acute stage of Stevens-Johnson syndrome and toxic epidermal necrolysis: a cross-sectional study. *BMC Ophthalmol.* **23**, 1–14 (2023).
13. Metcalfe, D., Iqbal, O., Chodosh, J., Bouchard, C. S. & Saeed, H. N. Acute and Chronic Management of Ocular Disease in Stevens Johnson Syndrome/Toxic Epidermal Necrolysis in the USA. *Front. Med. (Lausanne).* **8**, 662897 (2021).
14. Gun, E. & Ozer, E. Corneal Histopathology in Stevens-Johnson Syndrome: A Case Report and Review of Literature. *SN Comprehensive Clinical Medicine 2022 4:1* **4**, 122- (2022).
15. Yoshikawa, Y. *et al.* Long-term Progression of Ocular Surface Disease in Stevens-Johnson Syndrome and Toxic Epidermal Necrolysis. *Cornea* **39**, 745–753 (2020).

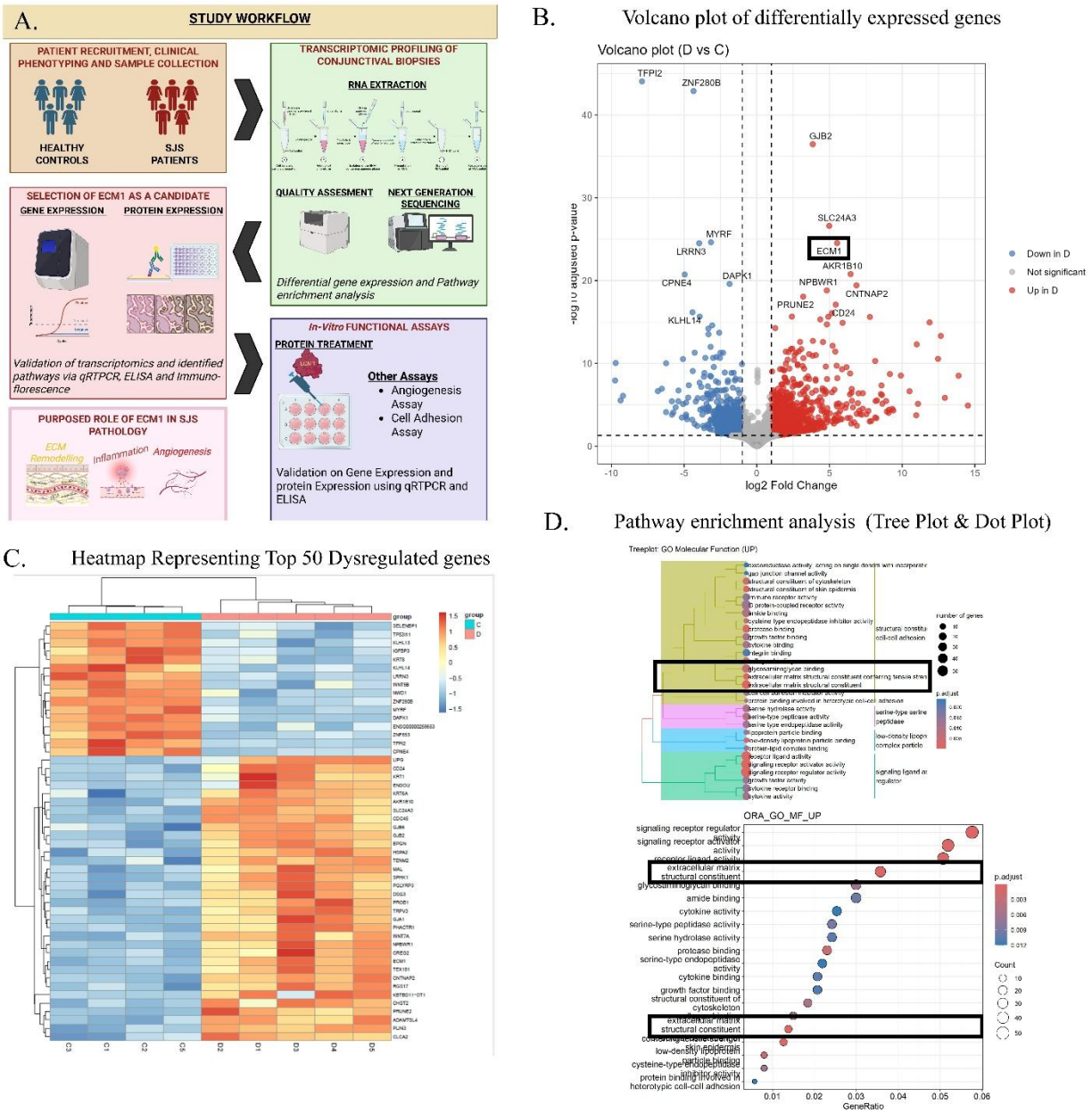
16. Kempuraj, D. & Mohan, R. R. Autophagy in Extracellular Matrix and Wound Healing Modulation in the Cornea. *Biomedicines 2022, Vol. 10,* **10**, (2022).
17. Wiemann, S., Reinhard, J. & Faissner, A. Immunomodulatory role of the extracellular matrix protein tenascin-C in neuroinflammation. *Biochem. Soc. Trans.* **47**, 1651–1660 (2019).
18. Kobayashi, Y. *et al.* Tenascin-C promotes angiogenesis in fibrovascular membranes in eyes with proliferative diabetic retinopathy. *Mol. Vis.* **22**, 436 (2016).
19. Panthagani, J. *et al.* Conjunctival transcriptomics in ocular mucous membrane pemphigoid. *Ocul. Surf.* **30**, 142–149 (2023).
20. Hardy, S. A. *et al.* Extracellular Matrix Protein-1 as a Mediator of Inflammation-Induced Fibrosis After Myocardial Infarction. *JACC Basic Transl. Sci.* **8**, 1539–1554 (2023).
21. Gijs, M. *et al.* Tear Fluid Inflammatory Proteome Analysis Highlights Similarities Between Keratoconus and Allergic Conjunctivitis. *Invest. Ophthalmol. Vis. Sci.* **64**, 9–9 (2023).
22. Leonardi, A., Borghesan, F., Depaoli, M., Plebani, M. & Secchi, A. G. Procollagens and inflammatory cytokine concentrations in tarsal and limbal vernal keratoconjunctivitis. *Exp. Eye Res.* **67**, 105–112 (1998).
23. Ninomiya, I. *et al.* Role of Oncostatin M in the Pathogenesis of Vernal Keratoconjunctivitis: Focus on the Barrier Function of the Epithelium and Interleukin-33 Production by Fibroblasts. *Invest. Ophthalmol. Vis. Sci.* **63**, 26 (2022).
24. Oyama, N. & Merregaert, J. The Extracellular Matrix Protein 1 (ECM1) in Molecular-Based Skin Biology. *Textbook of Aging Skin* 1–20 (2015) doi:10.1007/978-3-642-27814-3_8-2.
25. Sercu, S., Oyama, N. & Merregaert, J. *Importance of Extracellular Matrix Protein 1 (ECM1) in Maintaining the Functional Integrity of the Human Skin*. *The Open Dermatology Journal* vol. 3 (2009).
26. Zhang, Y. *et al.* ECM1 is an essential factor for the determination of M1 macrophage polarization in IBD in response to LPS stimulation. *Proc. Natl. Acad. Sci. U. S. A.* **117**, 3083–3092 (2020).
27. Sercu, S. *et al.* Interaction of Extracellular Matrix Protein 1 with Extracellular Matrix Components: ECM1 Is a Basement Membrane Protein of the Skin. *Journal of Investigative Dermatology* **128**, 1397–1408 (2008).
28. Zhao, J. *et al.* Mechanistic study of celastrol-mediated inhibition of proinflammatory activation of macrophages in IgA nephropathy via down-regulating ECM1. *Int. J. Biol. Sci.* **20**, 5731–5746 (2024).
29. Ye, H. *et al.* MiR-486-3p targeting ECM1 represses cell proliferation and metastasis in cervical cancer. *Biomedicine & Pharmacotherapy* **80**, 109–114 (2016).
30. Li, Y. *et al.* ECM1 expression in chronic liver disease: Regulation by EGF/STAT1 and IFNγ/NRF2 signalling. *JHEP Reports* **7**, (2025).
31. Fujimoto, M. *et al.* Myeloperoxidase-positive mononuclear cells predominate over CD3-positive T-lymphocytes in the epidermis of Stevens–Johnson syndrome and toxic epidermal necrolysis. *Virchows Archiv 2025* 1–6 (2025) doi:10.1007/S00428-025-04279-Z.
32. Koduri, M. A. *et al.* Neutrophil-driven and interleukin-36γ-associated ocular surface inflammation in chronic Stevens–Johnson syndrome. *Allergy: European Journal of Allergy and Clinical Immunology* **79**, 2128–2143 (2024).

33. Kanehisa, M., Furumichi, M., Sato, Y., Matsuura, Y. & Ishiguro-Watanabe, M. KEGG: biological systems database as a model of the real world. *Nucleic Acids Res.* **53**, D672–D677 (2025).
34. Home - Reactome Pathway Database. https://reactome.org/.
35. Szklarczyk, D. *et al.* The STRING database in 2023: protein-protein association networks and functional enrichment analyses for any sequenced genome of interest. *Nucleic Acids Res.* **51**, D638–D646 (2023).
36. Kitazawa, K. *et al.* Gene expression signatures of human senescent corneal and conjunctival epithelial cells. *Aging* **15**, 9238–9249 (2023).
37. Kojima, K. *et al.* Human conjunctival epithelial cells express functional Toll-like receptor 5. *Br. J. Ophthalmol.* **92**, 411–416 (2008).

## 11. Figure Captions

**Figure 1. Transcriptomic profiling reveals dysregulation in chronic ocular Stevens–Johnson syndrome** (A) Schematic overview of the study workflow. Conjunctival tissues obtained from chronic ocular Stevens–Johnson syndrome patients and healthy controls underwent bulk RNA sequencing followed by transcriptomic analysis, pathway enrichment, molecular validation, and in vitro functional assays to investigate the role of ECM1 in chronic ocular SJS pathology. (B) Volcano plot demonstrating significantly dysregulated genes between chronic ocular SJS conjunctiva and healthy controls. Differential gene expression analysis identified 2978 significantly dysregulated genes (adjusted p-value < 0.05), including upregulation of extracellular matrix-associated and inflammatory genes such as ECM1. (C) Heatmap representing the top 50 dysregulated genes demonstrating distinct transcriptomic segregation between healthy and diseased conjunctival tissues. (D) Gene Set Enrichment Analysis (GSEA)-based pathway enrichment analysis demonstrating significant enrichment of extracellular matrix structural constituent pathways, extracellular matrix organization, cytokine activity, receptor-ligand signalling, growth factor binding, cell-cell adhesion, and protease-associated pathways in chronic ocular SJS conjunctiva.

595 .




596

597 **Figure 2. Validation of extracellular matrix remodelling and inflammatory alterations in**

598 **chronic ocular Stevens–Johnson syndrome**

599 **(A)** Heatmap showing differential expression of extracellular matrix (ECM) remodelling-

600 associated genes in conjunctival tissues from patients with chronic ocular Stevens–Johnson

601 syndrome (SJS) and healthy controls. **(B)** qRT-PCR validation in an independent cohort

demonstrating increased expression of *ECM1, TNC, FN1, ACTA2, MMP3, MMP9, SERPINE1,* and *TGFB1* in chronic ocular SJS conjunctival tissues compared with healthy controls (SJS, n = 20; healthy, n = 10). **(C)** Representative immunofluorescence images showing increased ECM1, TNC, and FN1 protein expression in chronic ocular SJS conjunctival tissues compared with healthy controls, with corresponding quantification of mean fluorescence intensity. **(D)** ELISA analysis of tear samples demonstrating increased levels of ECM1, TNC, IL-1β, and TNF-α in chronic ocular SJS compared with healthy controls (SJS, n = 15; healthy, n = 10). **(E)** Gelatin zymography of tear samples demonstrating increased matrix metalloproteinase-associated gelatinolytic activity in chronic ocular SJS, with densitometric quantification relative to healthy controls. Data are presented as mean ± SEM. Statistical comparisons between two groups were performed using the Mann–Whitney U test. $P < 0.05$, $\mathbf{P} < 0.01$, $\boldsymbol{P} < 0.001$.

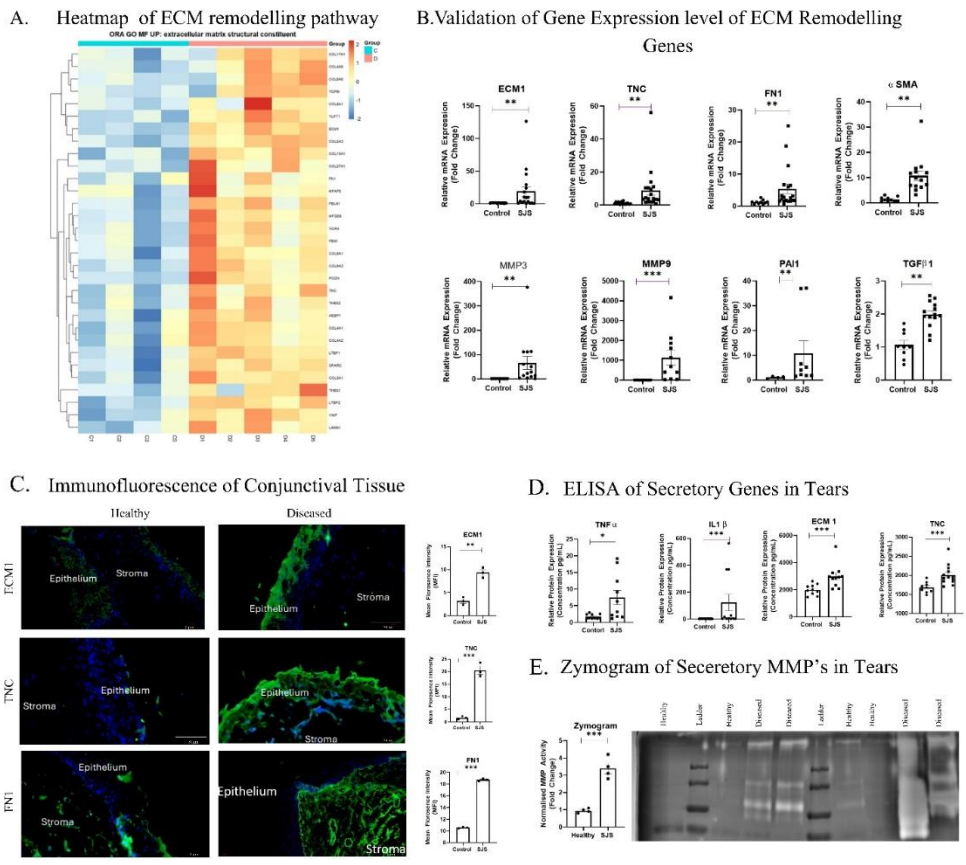
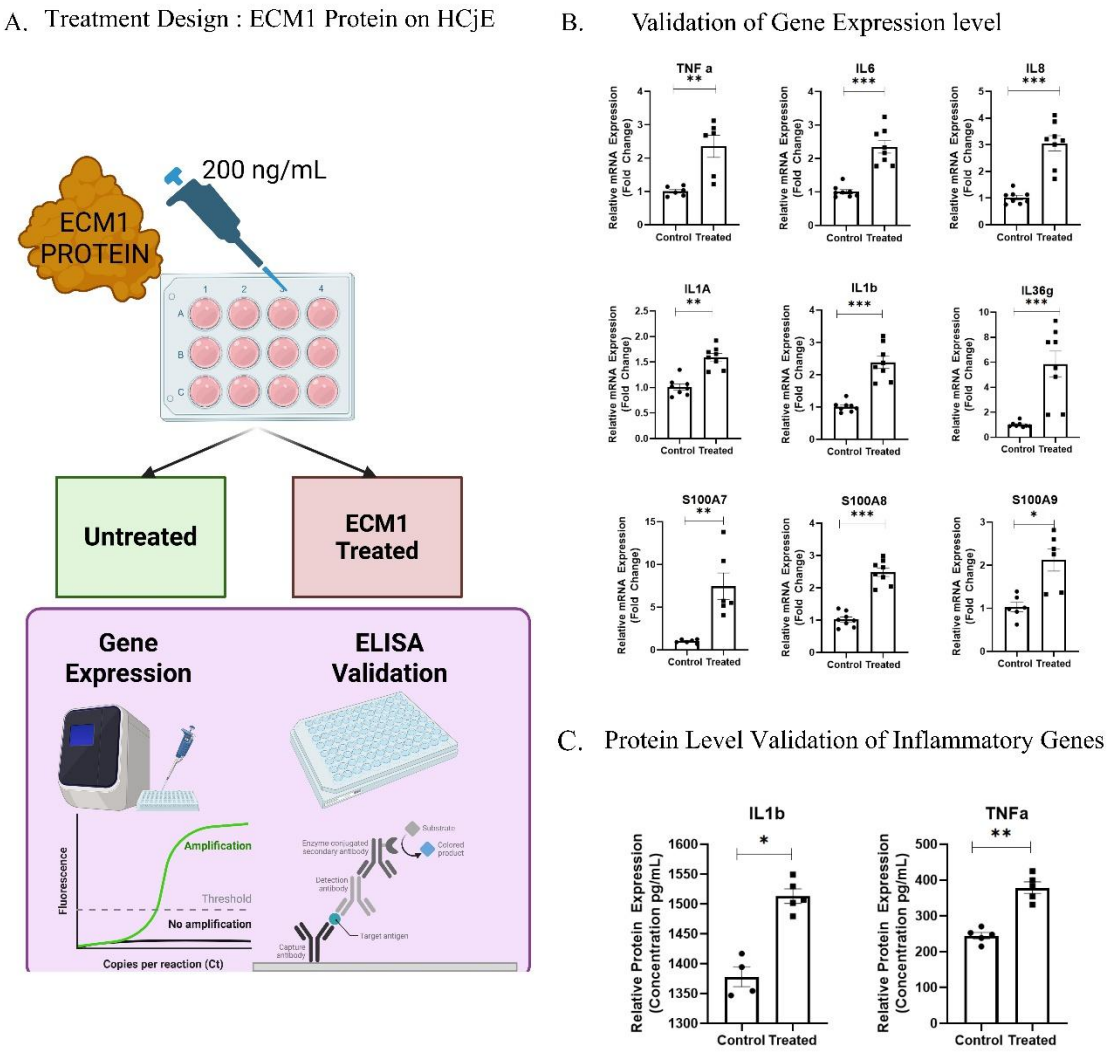


**Figure 3. ECM1 induces inflammatory responses in human conjunctival epithelial cells** (A) Experimental design illustrating recombinant ECM1 protein treatment of human conjunctival epithelial cells (HCjE) followed by downstream gene expression and ELISA-based protein validation analyses. (B) qRT-PCR analysis demonstrating increased expression of inflammatory mediators including TNFα, IL6, IL8, IL1A, IL1β, IL36γ, S100A7, S100A8, and S100A9 following ECM1 treatment compared to untreated controls. (C) ELISA-based protein validation demonstrating increased secretion of IL1β and TNFα following ECM1 treatment in HCjE cells. Data are represented as mean ± SEM. *$p < 0.05$, **$p < 0.01$, ***$p < 0.001$.




622

623 **Figure 4. ECM1 promotes adhesive and angiogenic responses in vitro** (A) Experimental
624 workflow illustrating ECM1-mediated functional assays including cell adhesion and angiogenesis
625 assays. (B) Cell adhesion assay performed using HCjE cells showed increased adhesion to ECM1-
626 coated surfaces compared with BSA-coated negative-control surfaces.. Representative brightfield
627 and fluorescence (Invitrogen™ Phalloidin Labeling Probes, Cat. No. A12379) images are shown
628 alongside quantitative fold-change analysis. (C) HUVEC tube formation assay demonstrating

ECM1-mediated angiogenic responses. Representative images demonstrate enhanced capillary-like network formation following ECM1 treatment at increasing concentrations compared to untreated controls. Quantitative analysis of junction number and segment length demonstrated increased angiogenic activity in ECM1-treated conditions. Data are represented as mean ± SEM. *p < 0.05, **p < 0.01, ***p < 0.001.

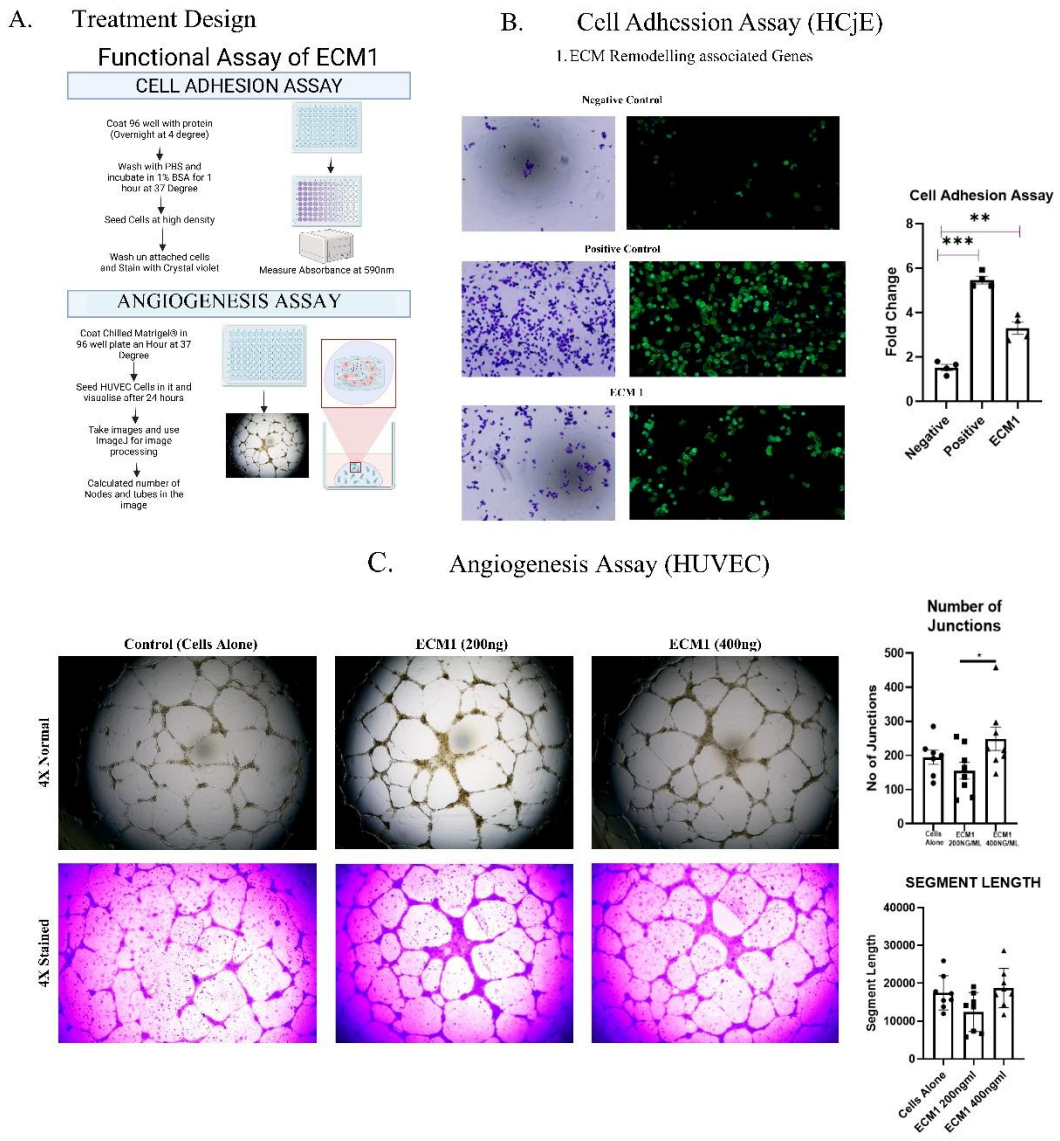
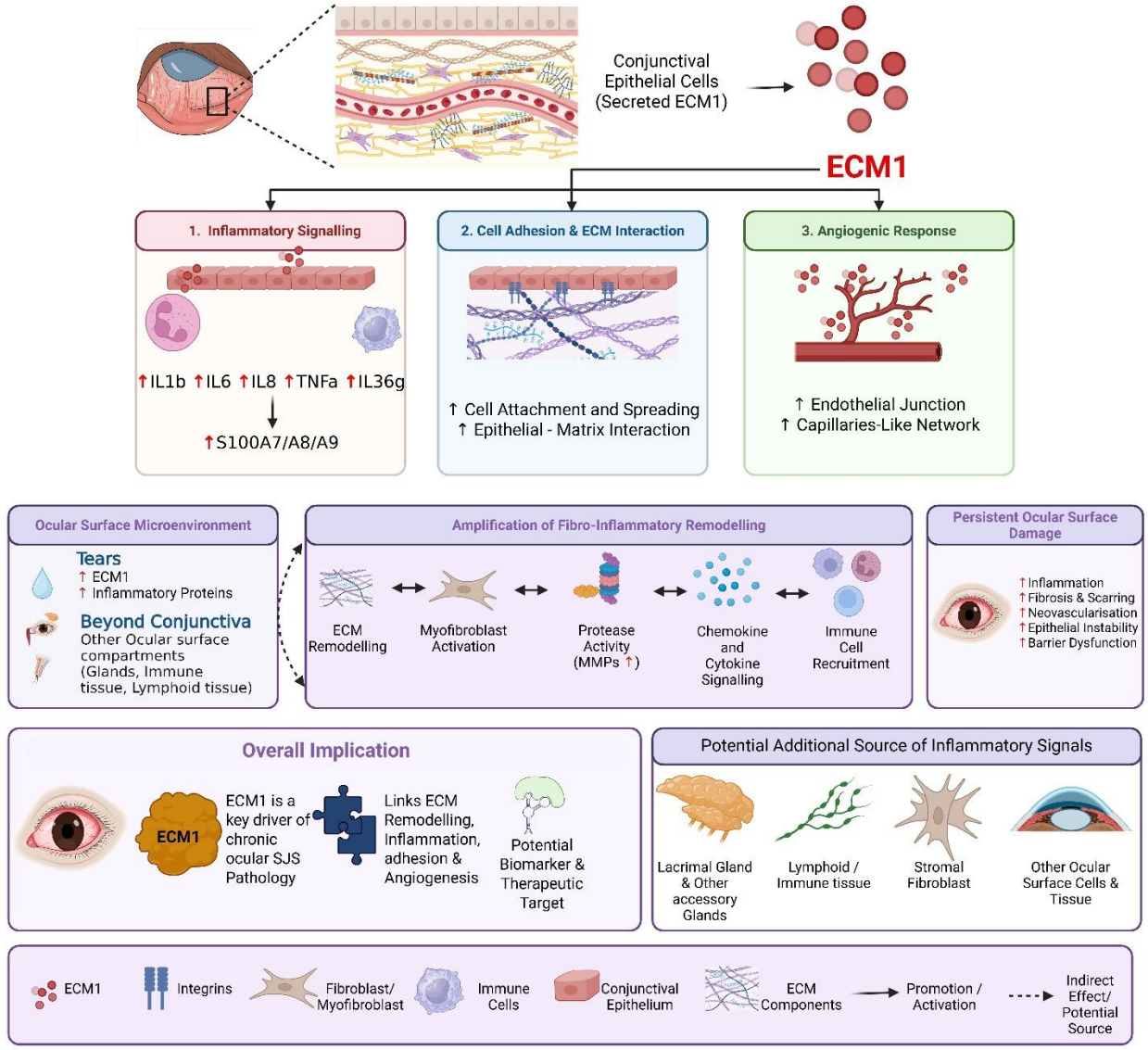



**Figure 5. Proposed model of ECM1-associated responses in chronic ocular SJS.** Increased ECM1 expression within the conjunctival microenvironment promotes inflammatory signaling,

ECM remodeling, epithelial–matrix interactions, and angiogenic responses, collectively contributing to persistent inflammatory ocular surface damage and disease progression in chronic ocular SJS.

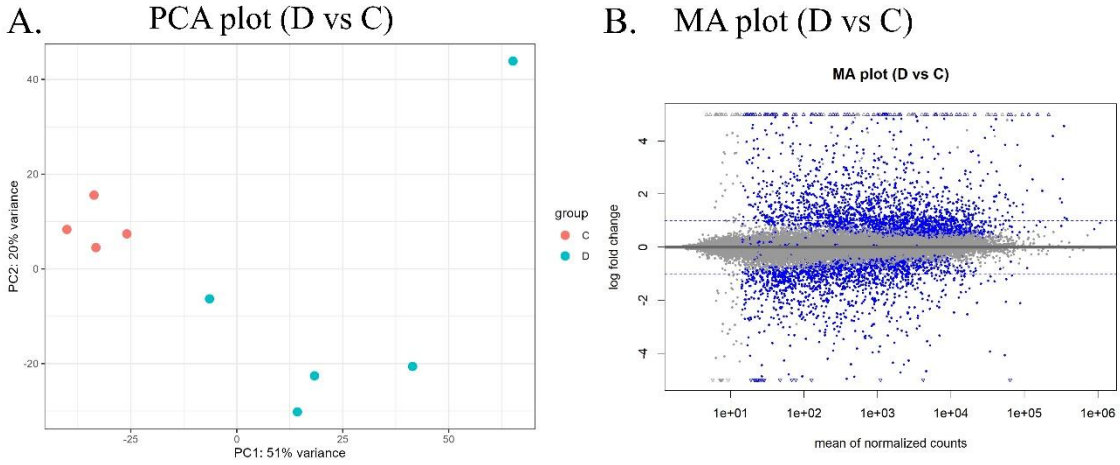



## 12. Supplementary Files

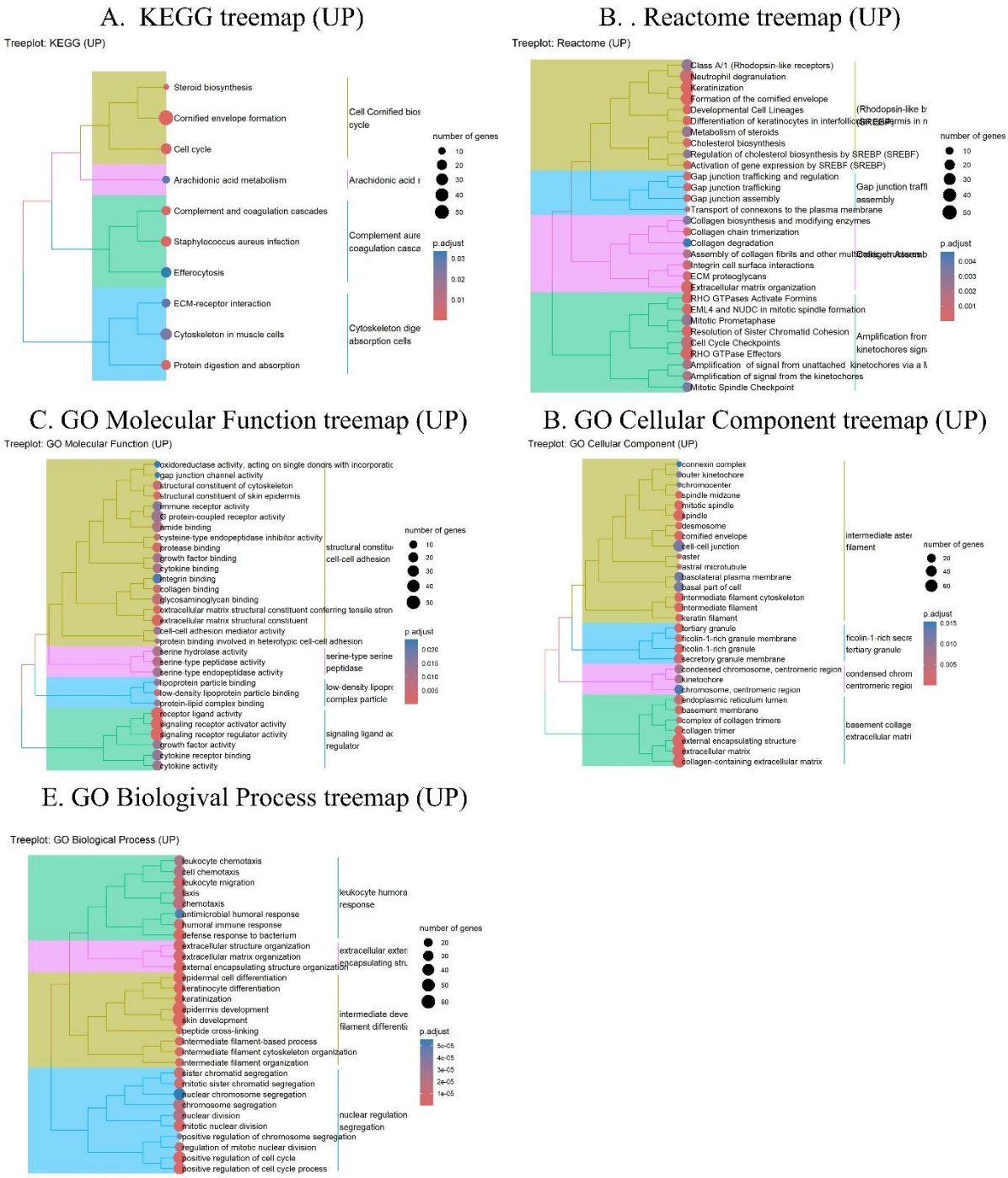
**Supplementary figure 1: Transcriptomic profiling of chronic ocular Stevens–Johnson syndrome.**

**(A)** Principal component analysis (PCA) of healthy control (C) and chronic ocular SJS (D) conjunctival tissues showing distinct clustering between groups. PC1 and PC2 explained 51% and 20% of the total variance, respectively. **(B)** MA plot showing differential gene expression between

chronic ocular SJS and healthy controls. Blue points represent significantly differentially expressed genes, while grey points indicate non-significant genes. These findings demonstrate substantial transcriptomic differences associated with chronic ocular SJS.

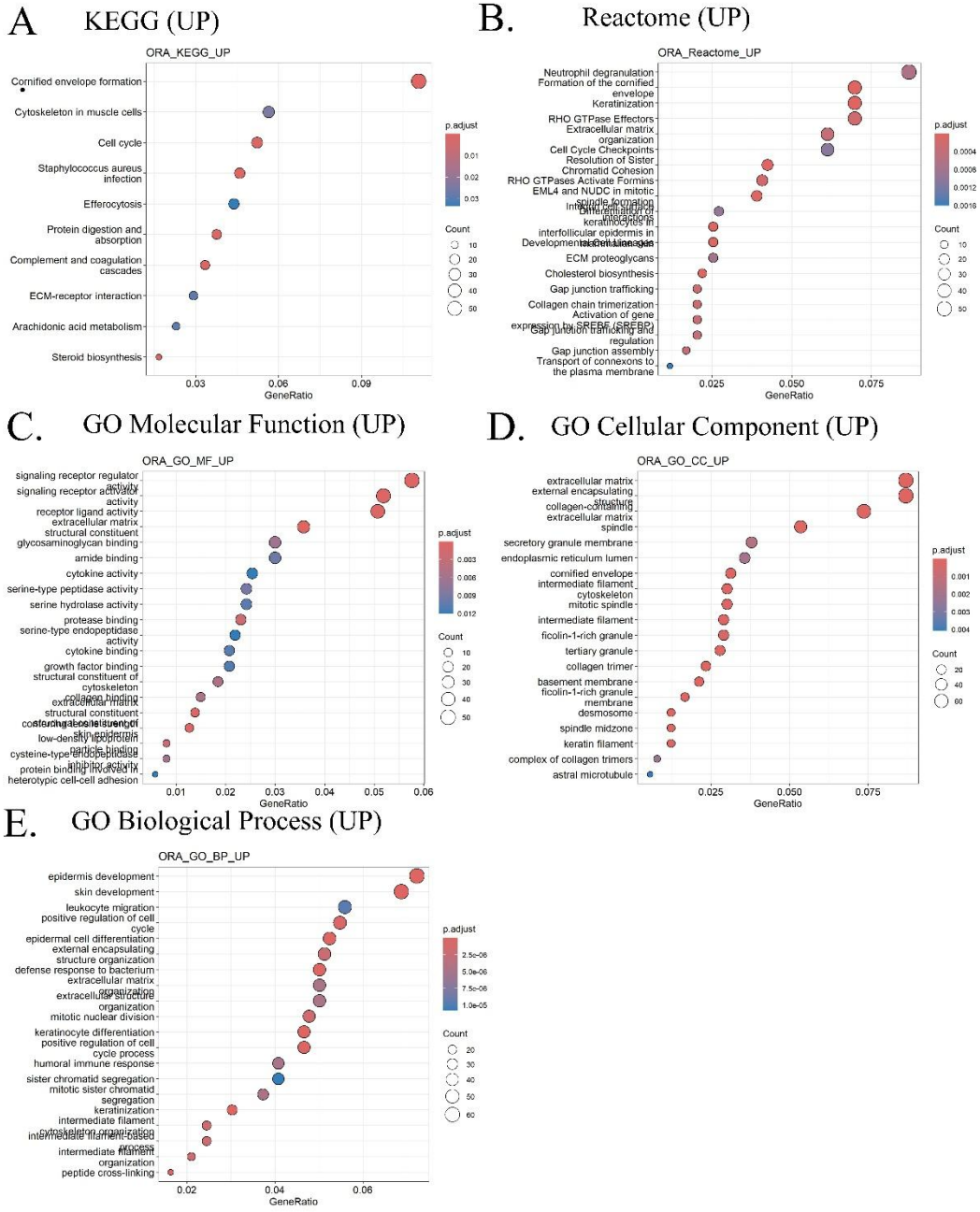



**Supplementary Figure 2. Functional enrichment analysis of upregulated genes in chronic ocular Stevens–Johnson syndrome.** Treemap-based enrichment analysis of significantly upregulated genes showing the major biological pathways and functional categories associated with chronic ocular SJS. **(A)** KEGG pathway enrichment, **(B)** Reactome pathway enrichment, **(C)** Gene Ontology (GO) Molecular Function enrichment, **(D)** GO Cellular Component enrichment, and **(E)** GO Biological Process enrichment. Enriched pathways were predominantly associated with extracellular matrix organization, cell adhesion, cytokine activity, keratinization, immune responses, extracellular matrix–receptor interactions, and tissue remodelling, highlighting extensive fibro-inflammatory alterations in chronic ocular SJS conjunctiva.



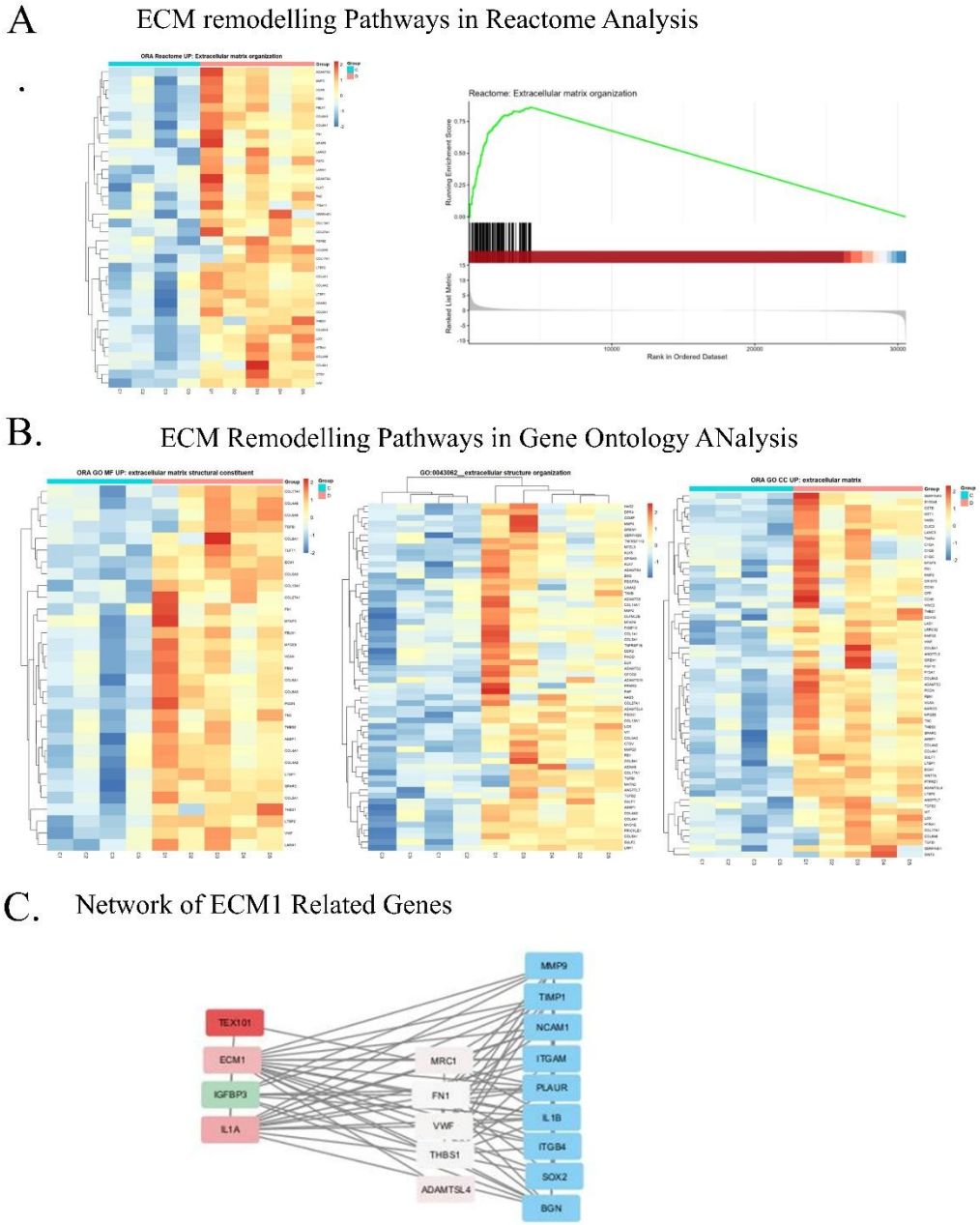

**Supplementary Figure 3. Over-representation analysis (ORA) of upregulated genes in chronic ocular Stevens–Johnson syndrome.** Dot plots showing significantly enriched pathways and Gene Ontology (GO) terms among upregulated genes in chronic ocular SJS conjunctival tissues. **(A)** KEGG pathway enrichment, **(B)** Reactome pathway enrichment, **(C)** GO Molecular Function enrichment, **(D)** GO Cellular Component enrichment, and **(E)** GO Biological Process enrichment. Enriched categories were predominantly related to extracellular matrix organization, keratinization, cytokine activity, cell

adhesion, neutrophil-associated responses, epithelial differentiation, and tissue remodelling, supporting the presence of persistent fibro-inflammatory alterations in chronic ocular SJS.



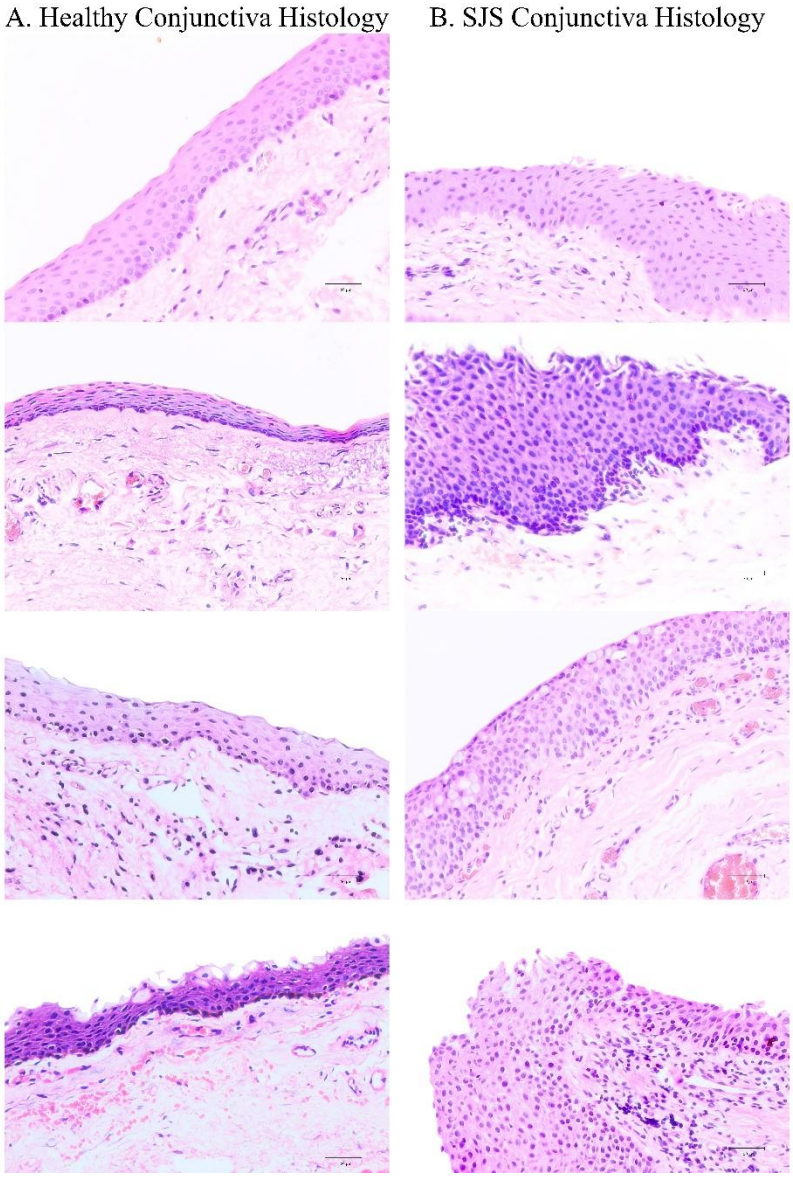

**Supplementary Figure 4. Extracellular matrix (ECM) remodelling-associated pathways and ECM1 interaction network in chronic ocular Stevens–Johnson syndrome. (A)** Reactome pathway analysis highlighting enrichment of extracellular matrix organization pathways in chronic ocular SJS. Representative heatmap demonstrates differential expression of ECM-associated genes between healthy controls and diseased conjunctival tissues, while Gene Set Enrichment Analysis (GSEA) confirms significant enrichment of extracellular matrix organization pathways in diseased

samples. **(B)** Gene Ontology (GO) enrichment analyses of extracellular matrix-related categories, including extracellular matrix structural constituent (Molecular Function), extracellular structure organization (Biological Process), and extracellular matrix (Cellular Component). Heatmaps illustrate coordinated upregulation of ECM-associated genes in chronic ocular SJS tissues. **(C)** Protein–protein interaction network of ECM1-associated genes generated from transcriptomic data, demonstrating interactions between ECM1 and multiple extracellular matrix, inflammatory, and remodelling-related molecules, supporting a central role for ECM1 within fibro-inflammatory remodelling pathways in chronic ocular SJS.

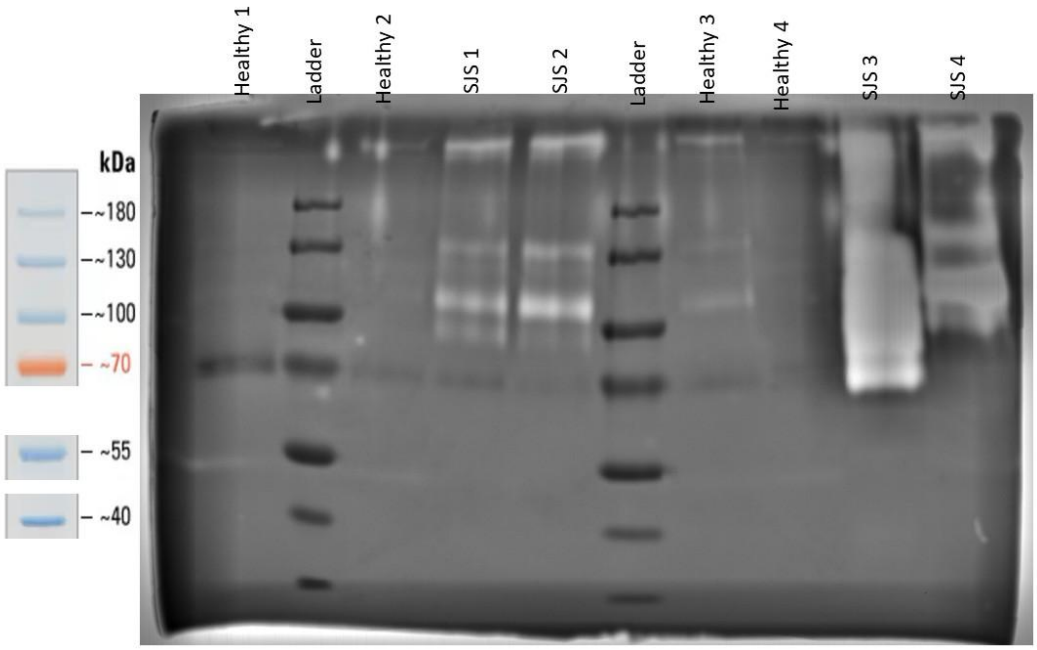



**Supplementary Figure 5. Histopathological features of healthy and chronic ocular Stevens–Johnson syndrome conjunctival tissues.** Representative hematoxylin and eosin (H&E)-stained sections of conjunctival tissues from healthy controls (A) and chronic ocular Stevens–Johnson syndrome (SJS) patients (B). Healthy conjunctiva demonstrates a relatively thin, well-organized

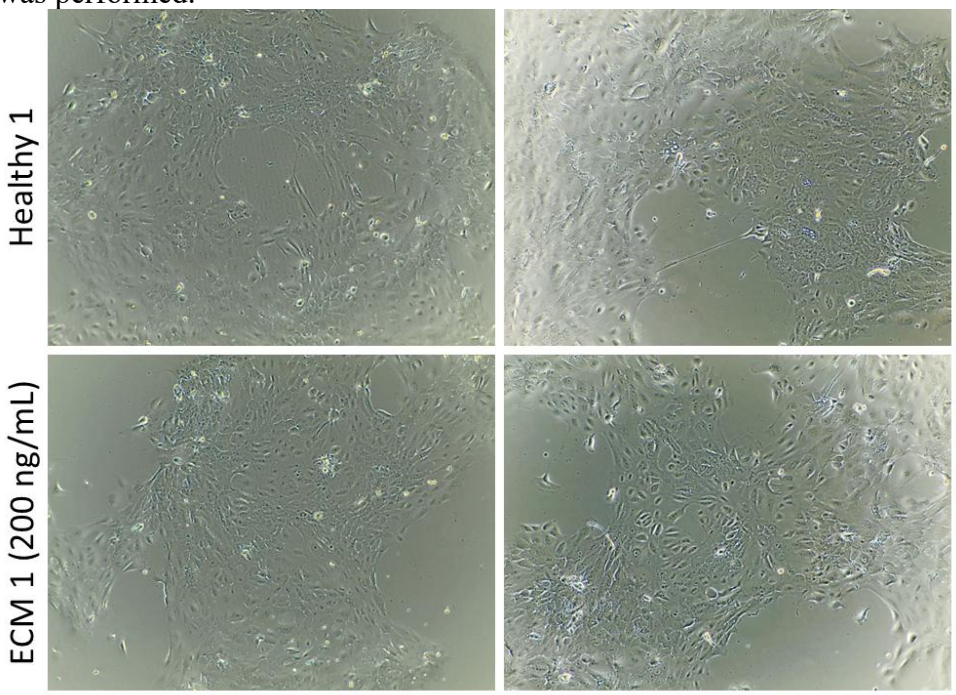
epithelial layer with minimal inflammatory cell infiltration and preserved stromal architecture. In contrast, SJS conjunctival tissues exhibit epithelial thickening (hyperplasia), increased cellularity, and prominent inflammatory cell infiltration within the epithelial and subepithelial compartments, accompanied by stromal remodelling and tissue disorganization. These findings are consistent with the chronic inflammatory and remodelling phenotype observed in ocular SJS.




**Supplementary Figure 6. Gelatin zymography of tear samples from healthy controls and patients with chronic ocular Stevens–Johnson syndrome.** Representative gelatin zymogram showing gelatinolytic activity in tear samples from individual healthy controls (Healthy 1–4) and patients with chronic ocular Stevens–Johnson syndrome (SJS 1–4). Molecular-weight protein ladders were included between sample groups, with approximate molecular weights indicated in kilodaltons (kDa). Areas of gelatin degradation represent gelatinase-associated proteolytic activity. Each numbered lane represents an individual participant sample.




**Supplementary Figure 7. Representative morphology of human conjunctival epithelial cells following ECM1 exposure.** Representative phase-contrast images of cultured human conjunctival epithelial (HCjE) cells under untreated control conditions (Healthy 1) and following treatment with recombinant ECM1 (200 ng/mL) for 24 h. Two representative microscopic fields are shown for each condition. Images were acquired under comparable culture and imaging conditions to document cellular morphology following ECM1 exposure. No quantitative morphological analysis was performed.




**Supplementary Table 1. Demographic and clinical characteristics of patients with chronic ocular Stevens–Johnson syndrome (SJS) and toxic epidermal necrolysis (TEN):** The table

summarizes the demographic and clinical details of the study cohort, including patient age, sex, duration of disease since the acute episode (years), and clinical diagnosis. The cohort comprised patients with chronic ocular manifestations of Stevens–Johnson syndrome (SJS), toxic epidermal necrolysis (TEN), and one patient with TEN associated with secondary Sjögren's syndrome. Disease duration ranged from **0.3 to 56 years**, reflecting the long-term and heterogeneous nature of chronic ocular surface involvement in SJS/TEN. Ages are presented in years, and sex is indicated as male (M) or female (F).

| Code | Age | Years of SJS | Acute Stage Diagnosis | Grading |
|---|---|---|---|---|
| Patient 1 | 70/F | 3 | SJS | very severe |
| Patient 2 | 44/M | 2.5 | SJS | very severe |
| Patient 3 | 19/M | 0.6 | TEN | very severe |
| Patient 4 | 25/F | 9 | TEN | Moderate |
| Patient 5 | 10/F | 0.5 | TEN | Moderate |
| Patient 6 | 50/F | 3 | SJS | Severe |
| Patient 7 | 61/F | 32 | TEN | very severe |
| Patient 8 | 15/F | 2 | TEN | moderate |
| Patient 9 | 68/F | 3 | SJS | very severe |
| Patient 10 | 35/M | 7 | TEN | very severe |
| Patient 11 | 54/M | 51 | SJS | Severe |
| Patient 12 | 16/F | 5 | TEN | Moderate |
| Patient 13 | 46/M | 4 | TEN | Moderate |
| Patient 14 | 62/F | 56 | TEN | severe |
| Patient 15 | 30/M | 27 | TEN | severe |
| Patient 16 | 64/F | 3 | SJS | mild |
| Patient 17 | 64/M | 21 | TEN | severe |
| Patient 18 | 35/M | 30 | TEN | Severe |
| Patient 19 | 29/F | 7 | TEN | Moderate |
| Patient 20 | 31/F | 5 | TEN | Moderate |
| Patient 21 | 40/M | 25 | SJS | Severe |
| Patient 22 | 8/M | 0.3 | TEN | very severe |
| Patient 23 | 44/M | 6 | TEN | very severe |
| Patient 24 | 42/F | 2 | SJS | very severe |
| Patient 25 | 21/F | 14 | SJS | Moderate |

**Supplementary Table 2. Primer sequences used for quantitative real-time PCR (qRT-PCR) analysis.**

| Gene | Forward (5'-3') | Reverse (5'-3') |
|---|---|---|
| **ECM1** | GCTTCACGGCTACAGGACAG | GAGGCTTCGGGATAGGGGT |
| **FN1** | CCC AAC TGG CAT TGA CTT TT | CTC GAG GTC TCC CAC TGA AG |
| **TNC** | TCCCAGTGTTCGGTGGATCT | TTGATGCGATGTGTGAAGACA |

| | | |
|---|---|---|
| **αSMA** | TGGCTATTCCTTCGTTACTACTGCT | CATCAGGCAACTCGTAACTCTTCTC |
| **MMP3** | CTGGACTCCGACACTCTGGA | CAGGAAAGGTTCTGAAGTGACC |
| **MMP9** | GCGTCGTGATCCCCACTTAC | CAGGCCGAATAGGAGCGTC |
| **PAI1** | AGTGGACTTTTCAGAGGTGGA | GCCGTTGAAGTAGAGGGCATT |
| **TGFβ1** | TGAACCGGCCTTTCCTGCTTCTCATG | GCGGAAGTCAATGTACAGCTGCCGC |
| **IL1α** | AGATGCCTGAGATACCCAAAACC | CCAAGCACACCCAGTAGTCT |
| **IL1β** | ATGATGGCTTATTACAGTGGCAA | GTCGGAGATTCGTAGCTGGA |
| **IL6** | ACTCACCTCTTCAGAACGAATTG | CCATCTTTGGAAGGTTCAGGTTG |
| **IL36γ** | AAGTGACAGTGTGACCCCAGT | GGATTCTGGATTCCCAAATAAA |
| **TNFα** | CAAGGACAGCAGAGGACCAG | TCCTTTCCAGGGGAGAGAGG |
| **S100A7** | ACGTGATGACAAGATTGACAAGC | GCGAGGTAATTTGTGCCCTTT |
| **S100A8** | ATGCCGTCTACAGGGATGAC | ACGCCCATCTTTATCACCAG |
| **S100A9** | GTGCGAAAAGATCTGCAAAA | TCAGCTGCTTGTCTGCATTT |

728